World Academy of Science, Engineering and Technology
International Journal of Aerospace and Mechanical Engineering
Vol:16, No:3, 2022

Utilization of Schnerr-Sauer Cavitation Model for Simulation of Cavitation Inception and Super Cavitation

Mohammadreza Nezamirad, Azadeh Yazdi, Sepideh Amirahmadian, Nasim Sabetpour, Amirmasoud Hamedi

***Abstract*—**In this study, the Reynolds-Stress-Navier-Stokes framework is utilized to investigate the flow inside the diesel injector nozzle. The flow is assumed to be multiphase as the formation of vapor by pressure drop is visualized. For pressure and velocity linkage, the coupled algorithm is used. Since the cavitation phenomenon inherently is unsteady, the quasi-steady approach is utilized for saving time and resources in the current study. Schnerr-Sauer cavitation model is used, which was capable of predicting flow behavior both at the initial and final steps of the cavitation process. Two different turbulent models were used in this study to clarify which one is more capable in predicting cavitation inception and super-cavitation. It was found that K-ε was more compatible with the Shnerr-Sauer cavitation model; therefore, the mentioned model is used for the rest of this study.

***Keywords*—**CFD, RANS, cavitation, fuel, injector.

I.INTRODUCTION

CAVITATION is the phenomenon in which pressure drops very fast, and as the result of a steep pressure drop, the vapor region forms. The main advantage of cavitation phenomena is the formation of a two-phase flow inside the injector of the nozzle. Cavitation created inside the nozzle augments turbulence value which has a contribution to primary jet breakup, atomization, and combustion [1], [2]. Cavitation bubbles are very vibrant and go through oscillation, coalescence, cloud or cluster formation, and collapse in which bubble collapse, which is the last step of cavitation, is the most detrimental one that causes malfunction among several equipments [3]-[6]. Since the behavior of the flow inside the nozzle has a significant effect on the combustion and spray process, understanding the internal flow inside the nozzle is crucial in order to reduce pollutants as much as we can [7]-[9]. The occurrence of cavitation inside the nozzle is a very useful phenomenon as it can be controlled by injection pressure or even outlet pressure [10], [11]. Streamline contraction leads to narrowing velocity profile by decreasing the effective cross-section of the flow passing the injector [12]-[14].

Several computational and experimental investigations are reported that are focusing on cavitation inception, supercavitation, and the two-phase flow inside diesel injector nozzle [15], [16]. In general, there are two approaches that are mainly used for the prediction of cavitation inside diesel injector nozzle, which are single continuum models that are used as average mixture properties and two-fluid models in which liquid and vapor phases are treated as two separate substances [17], [18]. Schmidt et al. [19] used thermal equilibrium for developing a model in which uniform distribution in each cell is utilized for the two phases. Afterward, using isentropic flow along with utilizing the Wallis approach, two-phase sound speed was modeled [20]. One of the major drawbacks of the single-phase approach is that turbulence is not considered comprehensively, which removes very crucial stochastic features from the flow. As mentioned earlier, in the two-fluid approach, vapor and liquid phases are considered as a combination of two forms of conservation equations. There are two major categories for the two-fluid model, which are the Eulerian-Eulerian approach and the Eulerian-Lagrangian approach [21].

In the present study, Winklhofer [22] rectangular shape nozzle is used to perform simulation and verification as the mentioned study has useful experimental data for making the comparison and also can be utilized for validation purposes. It is necessary to understand structure and formation in the near and internal nozzle region. Mostly, nozzles that are transparent are used to study cavitation behavior optically inside nozzles. In this study, the Winklhofer nozzle will be verified and validated for subsequent studies.

II.CAVITATION MODEL AND FORMULATION

Mostly cavitation is simulated using three main methods, which are the multiphase flow model, homogenous equilibrium model, and interface tracking model [9], [23]-[25]. In the current study, since the main focus is on severe variation of density, a multiphase flow model is selected in which real transformation is considered; hence, the Schenerr-Sauer cavitation model is used in the current investigation. The transport equation in the mentioned platform can be stated as following:

$$\frac{\partial}{\partial t}(\alpha.\rho_v) + \nabla(\alpha.\rho_v.\vec{V}_V) = \frac{\rho_v.\rho_l}{\rho}.\frac{d\alpha}{dt} \quad (1)$$

In (1), density of vapor is ρ_v, density of liquid is ρ_l, vapor volume fraction is α, velocity of gases phase is $\vec{V}_V$ and time is t. The relationship between density of liquid and density of vapor can be written as mass transfer equation which can be written as following:

Mohammadreza Nezamirad is with the University of South Florida, USA (e-mail: mnezamirad@usf.edu).

$$R = \frac{\rho_v.\rho_l}{\rho}.\frac{d\alpha}{dt} \quad (2)$$

Vapor volume fraction can be written as number of bubbles per unit of volume and radius of bubble as following:

$$\alpha = \frac{n_b \times \frac{4}{3} \times \pi R_b^{\ 3}}{1 + n_b \times \frac{4}{3} \times \pi R_b^{\ 3}} \quad (3)$$

in which R is the mass transfer between density of vapor and density of liquid, bubble radius is R_b. Finally, by adding (3) into (2), the following expression for mass transfer will be obtained:

$$\mathrm{R} = \frac{\rho_v.\rho_l}{\rho}.\alpha.(1-\alpha).\frac{3}{\mathrm{R_b}}.\sqrt{\frac{2}{3}.\left|\frac{p_v - p}{\rho_l}\right|} \quad (4)$$

$$\mathrm{R_b} = \left(\frac{\alpha}{1-\alpha}.\frac{3}{4.\pi}.\frac{1}{n}\right)^{\frac{1}{3}} \quad (5)$$

Also, p is static pressure of the far field and p_v is the static pressure of vapor.

Discharge coefficient can be written as an expression that includes mass flow rate and pressure difference.

$$\mathrm{Cd} = \frac{\dot{m}}{A\sqrt{2\rho_l(P_{in} - P_{back})}} \quad (6)$$

In (6) $\dot{m}$ is mass flow rate and area of the section of the nozzle that stated as A. Inlet pressure and outlet pressure are orderly P_{in} and P_{back}. Cavitation number (K) inside the nozzle can be defined as following:

$$\mathrm{K} = \frac{P_{in} - P_v}{P_{in} - P_{back}} \quad (7)$$

III. Geometry of the Domain

The rectangular shape nozzle introduced by Winklhofer et al. [22] is shown in Fig. 1. As the figure depicts, the inlet and outlet areas are assumed to be cubic shape in order to make the boundary condition closer to reality. The length of the orifice is 0.001 m, inlet area of the orifice is 301 μm by 300 μm, and outlet area of the orifice is 284 μm by 300 μm. The inlet radius of the orifice is 20 μm. The pressure inlet is fixed to 10 MPa and the pressure outlet is fixed to $2-5$ MPa. The turbulent intensity is $0.16 \times Re^{-1/8}$ for the inlet. Turbulent length scale for the inlet is defined as $0.07D$. Fig. 2 is showing the mesh topology used in this study. The mesh utilized in this work is quad dominant which means that the mesh is not fully structured, while it is mostly structured.

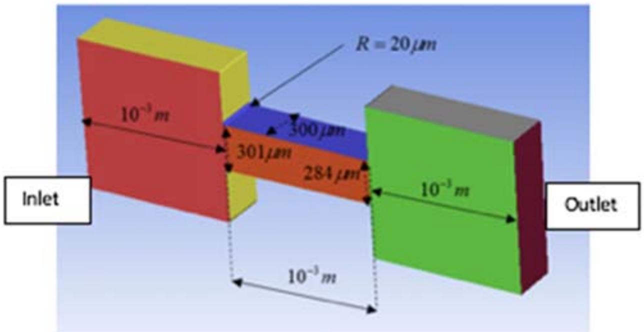

Fig. 1 Rectangular shape nozzle introduced by Winklhofer

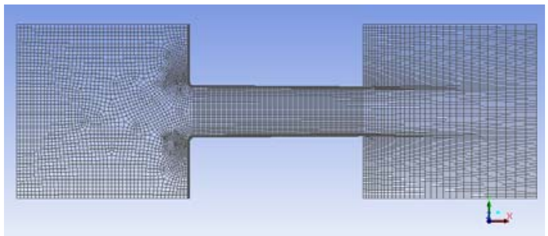

Fig. 2 Mesh for Winklhofer rectangular shape nozzle

IV. Result and Discussion

In this study, cavitation has been investigated both at the initial and final steps of formation. As can be seen in Fig. 3, when the simulated result is compared with the experimental result obtained by Winklhofer et al. [22] in both the initial and final stage of cavitation, the simulation was able to predict the formation of vapor volume fraction as described earlier in this study. When pressure drops down below the critical pressure, which is mostly vaporization pressure, cavitation starts to form, and then it continues to grow up in the orifice area until it reaches the end of the orifice area, which is called supercavitation. Further increase in pressure difference will end up in the formation of choke phenomena which is not favorable and affects the combustion process very adversely. Therefore, it is recommended to control the pressure difference until the flow reaches supercavitation, which helps the atomization process that is supposed to occur after cavitation.

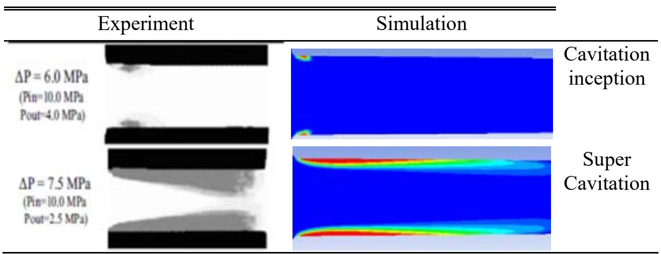

Fig. 3 Presentation of cavitation inception vs. super cavitation with vapor volume fraction

Velocity profile at a location of 53 μm from the orifice inlet is shown in Fig. 4, where the inlet pressure is fixed to 100 bar or 10 Mpa and the outlet pressure was chosen to be 45 bar and 33 bar separately. Two different turbulent models are utilized in this study, which are $K-\varepsilon$ and $K-\omega$ in order to select the most appropriate turbulent model while Reynolds Stress Navier Stokes (RANS) is utilized. As can be seen from Fig. 4, the average error obtained when $K-\varepsilon$ model was utilized, was 1.8% when compared to the experimental data, while the mentioned average error when $K-\varepsilon$ was utilized, was 7.2%, which shows the capability of $K-\varepsilon$ when cavitation simulation is of interest. Also, it can be seen from Fig. 4, that the current numerical approach was able to predict velocity profile trends at two different pressure differences that can be used as validation as well.

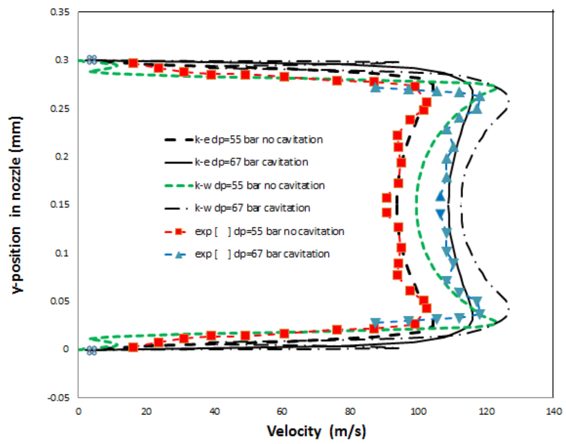

Fig. 4 Velocity profile at 53 μm from the orifice inlet at two different pressure differences which are 55 bar and 67 bar when the inlet pressure is fixed to 100 bar

Mass flow rate is shown at different pressure differences in Fig. 5 when two different turbulent approaches are utilized. It can be seen that the $k-\varepsilon$ turbulent approach comparing to $k-\omega$ has a better agreement with previous experimental data obtained by Winklhofer et al. [22].

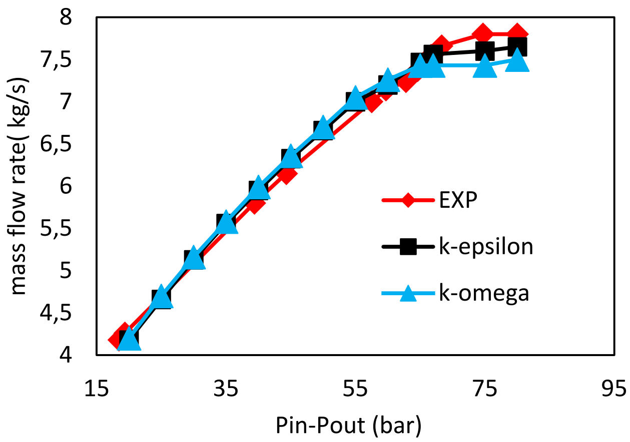

Fig. 5 Mass flow rate at different pressure differences when $k-\varepsilon$ and $k-\omega$ compared to experimental data obtained by winklhofer [22]

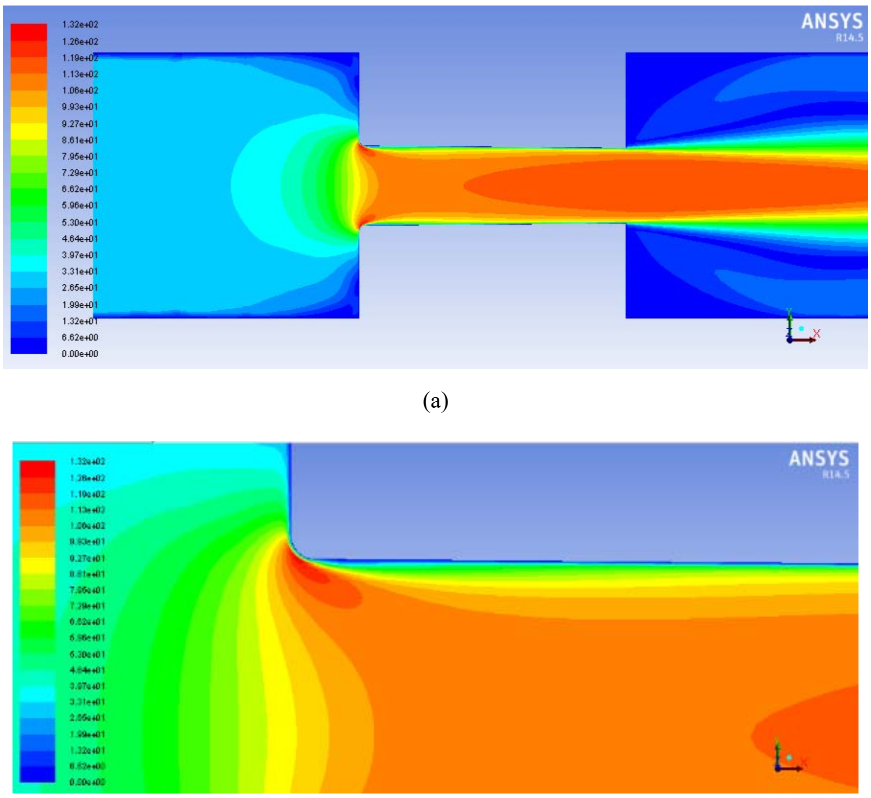

(a)

(b)

Fig. 6 Velocity distribution at mid plane when $\Delta p = 6\ Mpa$

Fig. 6 shows velocity distribution at the mid plane of the nozzle when $\Delta p = 6\ Mpa$. As the mentioned figure shows, the highest amount of velocity is observed at the mid orifice area and near the inlet area. The inlet area is also shown as a close-up view in Fig. 6 (b).

Fig. 7 is showing pressure distribution at the inlet of the nozzle. Since $\Delta p = 6\ Mpa$ is corresponding to the cavitation inception, a very narrow region of low-pressure zone which is indicating the formation of cavitation can be seen at the inlet of the orifice.

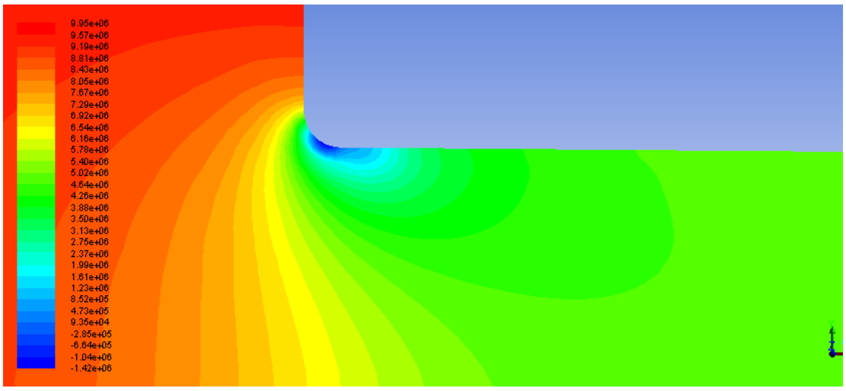

Fig. 7 Pressure distribution at mid plane when $\Delta p = 6\ Mpa$

V. Conclusion

In this study, flow inside the diesel injector nozzle is simulated in which a finite volume framework is utilized for solving RANS equations. Schnerr-Sauer cavitation model is used for simulating cavitation in multiphase flow. The carrying fluid in this study is diesel fuel, and other boundary conditions are following the experimental study for the verification purposes proposed by Winklhofer et al. [22]. The current numerical approach could successfully predict cavitation at both initial and final stages. $K-\omega$ and $K-\varepsilon$ turbulent approaches were both investigated, and it was found that results obtained using $K-\varepsilon$ have a better agreement with previous experimental data [26]-[31].

References

[1] Zeidi, S. and M. Mahdi, *Investigation the effects of injection pressure and compressibility and nozzle entry in diesel injector nozzle's flow.* Journal of Applied and Computational Mechanics, 2015. **1**(2): p. 83-94.

[2] Zeidi, S. M. J. and M. Mahdi, *Evaluation of the physical forces exerted on a spherical bubble inside the nozzle in a cavitating flow with an Eulerian/Lagrangian approach.* European Journal of Physics, 2015. **36**(6).

[3] Reuter, F., et al., *Wall Shear Rates Induced by a Single Cavitation Bubble Collapse*, in *Proceedings of the 10th International Symposium on Cavitation (CAV2018)*, J. Katz, Editor. 2018, ASME Press. p. 0.

[4] Salvador, F. J., et al., *Using a homogeneous equilibrium model for the study of the inner nozzle flow and cavitation pattern in convergent-divergent nozzles of diesel injectors.* Journal of Computational and Applied Mathematics, 2017. **309**: p. 630-641.

[5] Peters, A., U. Lantermann, and O. el Moctar, *Simulation of an Internal Nozzle Flow Using an Euler-Lagrange Method*, in *Proceedings of the 10th International Symposium on Cavitation (CAV2018)*, J. Katz, Editor. 2018, ASME Press. p. 0.

[6] Pearce, D., *Pressure waves and cavitation in diesel fuel injection rate characterisation*. 2017, Imperial College London.

[7] Fu, Y., Z. P. Xie, and W. G. Zhao, *Prediction Method of Cavitation Jet Wave Attenuation Based on Five-Equation Two-Fluid Model.* Mathematical Problems in Engineering, 2020. **2020**. M Nezamirad, S Amirahmadian, N Sabetpour, A Yazdi, A Hamedi, Effect of Different Diesel Fuels on Formation of the Cavitation Phenomena. International Journal of Aerospace and Mechanical Engineering, 2021. 15(7).

[8] Cristofaro, M., et al., *A numerical study on the effect of cavitation erosion in a diesel injector.* Applied Mathematical Modelling, 2020. **78**: p. 200-216.

[9] Vanhille, C., *Numerical simulations of stable cavitation bubble generation and primary Bjerknes forces in a three-dimensional nonlinear phased array focused ultrasound field.* Ultrasonics Sonochemistry, 2020. **63**.

[10] Sun, L. G., P. C. Guo, and X. Q. Luo, *Numerical investigation on inter-blade cavitation vortex in a Franics turbine.* Renewable Energy, 2020. **158**: p. 64-74.

[11] Chen, J., L. L. Geng, and X. Escaler, *Numerical Investigation of the Cavitation Effects on the Vortex Shedding from a Hydrofoil with Blunt Trailing Edge.* Fluids, 2020. **5**(4).

[12] Chiu, C. and C. F. Moss, *The role of the external ear in vertical sound localization in the free flying bat, Eptesicus fuscus.* Journal of the Acoustical Society of America, 2007. **121**(4).

[13] von Bayern, A. M. P., et al., *The role of experience in problem solving and innovative tool use in crows.* Current Biology, 2009. **19**(22): p. 1965-1968.

[14] Schnerr, G. H. and J. Sauer. *Physical and numerical modeling of unsteady cavitation dynamics.* in *Fourth international conference on multiphase flow*. 2001. ICMF New Orleans.

[15] Macian, V., et al., *A CFD analysis of the influence of diesel nozzle geometry on the inception of cavitation.* Atomization and Sprays, 2003. **13**(5-6): p. 579-604.

[16] Blessing, M., et al., *Analysis of flow and cavitation phenomena in diesel injection nozzles and its effects on spray and mixture formation.* Fuel Injection Systems, 2003. **2003**(2): p. 21-32.

[17] Hu, Q., Y. Yang, and W. Cao, *Computational analysis of cavitation at the tongue of the volute of a centrifugal pump at overload conditions.* Advances in Production Engineering & Management, 2020. **15**(3): p. 295-306.

[18] Geng, L. L. and X. Escaler, *Assessment of RANS turbulence models and Zwart cavitation model empirical coefficients for the simulation of unsteady cloud cavitation.* Engineering Applications of Computational Fluid Mechanics, 2020. **14**(1): p. 151-167.

[19] Schmidt, D. P., et al., *Cavitation in Two-Dimensional Asymmetric Nozzles.* 1999, SAE International.

[20] Nedderman, R.M., *One-Dimensional Two-Phase Flow. BY G. B. WALLIS. McGraw Hill, 1969. 408pp. £7. 18s. Cocurrent Gas-Liquid Flow. Edited by E. RHODES AND D. S. SCOTT. Plenum Press, 1969. 698 pp. $27.50.* Journal of Fluid Mechanics, 1970. **42**(2): p. 428-430.

[21] Singhal, A. K., et al., *Mathematical basis and validation of the full cavitation model.* J. Fluids Eng., 2002. **124**(3): p. 617-624.

[22] Winklhofer, E., et al. *Comprehensive hydraulic and flow field documentation in model throttle experiments under cavitation conditions*. in *Proceedings of the ILASS-Europe conference, Zurich*. 2001.

[23] Som, S., *Development and validation of spray models for investigating diesel engine combustion and emissions*. 2009: University of Illinois at Chicago.
[24] Xu, X. G., et al., *3D numerical investigation of energy transfer and loss of cavitation flow in perforated plates.* Engineering Applications of Computational Fluid Mechanics, 2020. **14**(1): p. 1095-1105.
[25] Yusvika, M., et al., *Cavitation Prediction of Ship Propeller Based on Temperature and Fluid Properties of Water.* Journal of Marine Science and Engineering, 2020. **8**(6).
[26] N. Sabetpour, A. Yazdi, S. Amirahmadian, M. Nezamirad, A. Hamedi, Formation of Vapor Volume Fraction in a real size nozzle using Schnerr and Sauer approach. Forth Conference on Technology Development in Mechanical and Aerospace Engineering, 2021.
[27] A. Yazdi, N. Sabetpour, S. Amirahmadian, M. Nezamirad, A. Hamedi, Effect of Pressure Difference and Needle Height on Formation of Cavitation in a real size nozzle. Forth Conference on Technology Development in Mechanical and Aerospace Engineering, 2021.
[28] M. Nezamirad, S. Amirahmadian, N. Sabetpour, A. Hamedi, A. Yazdi, Effect of Needle Height on Formation of Cavitation in a Six-Hole Diesel Injector Nozzle. 6th national conference on Mechanical and Aerospace Engineering, 2021.
[29] A. Yazdi, M. Nezamirad, S. Amirahmadian, N. Sabetpour, A. Hamedi, Effect of Needle Height on Discharge Coefficient and Cavitation Number. International Journal of Aerospace and Mechanical Engineering, 2021. 15(7).
[30] M. Nezamirad, S. Amirahmadian, N. Sabetpour, A. Yazdi, A. Hamedi, Effect of Different Diesel Fuels on Formation of the Cavitation Phenomena. International Journal of Aerospace and Mechanical Engineering, 2021. 15(7).
[31] M. Nezamirad, N. Sabetpour, A. Yazdi, A. Hamedi, Investigation the Effect of Velocity inlet and Carrying Fluid on the Flow inside Coronary Artery. International Journal of Aerospace and Mechanical Engineering, 2021. 15(7).